Nintedanib reduces radiation -induced microscopic lung fibrosis but this cannot be monitored by CT imaging

Radiotherapy and Oncology 124 (2017) 482–487

Contents lists available at ScienceDirect

Radiotherapy and Oncology

journal homepage: www.thegreenjournal.com

Experimental radiobiology

Nintedanib reduces radiation-induced microscopic lung fibrosis but this cannot be monitored by CT imaging: A preclinical study with a high precision image-guided irradiator ☆

Dirk De Ruysscher [a,b], Patrick Vincent Granton [a], Natasja Gaby Lieuwes [a], Stefan van Hoof [a], Lutz Wollin [c], Birgit Weynand [d], Anne-Marie Dingemans [e], Frank Verhaegen [a], Ludwig Dubois [a,*]

[a] Department of Radiation Oncology (Maastro), GROW – School for Oncology and Developmental Biology, Maastricht University Medical Center, The Netherlands; [b] Department of Radiation Oncology, KU Leuven, Belgium; [c] Boehringer Ingelheim Pharma GmbH & Co. KG, Biberach, Germany; [d] Department of Pathology, KU Leuven, Belgium; [e] Department of Pulmonology, GROW – School for Oncology and Developmental Biology, Maastricht University Medical Center, The Netherlands

ARTICLE INFO

Article history:
Received 1 May 2017
Received in revised form 14 July 2017
Accepted 14 July 2017
Available online 31 July 2017

Keywords:
Nintedanib
Radiation-induced lung damage
Radiation pneumonitis
Radiation fibrosis
Small animal image-guided precision irradiation

ABSTRACT

Background: Nintedanib has anti-fibrotic and anti-inflammatory activity and is approved for the treatment of idiopathic pulmonary fibrosis. The aim of this study was to noninvasively assess the efficacy of nintedanib in a mouse model of partial lung irradiation to prevent radiation-induced lung damage (RILD).

Methods: 266 C57BL/6 adult male mice were irradiated with a single radiation dose (0, 4, 8, 12, 16 or 20 Gy) using parallel-opposed fields targeting the upper right lung using a precision image-guided small animal irradiator sparing heart and spine based on micro-CT images. One week post irradiation, mice were randomized across nintedanib daily oral gavage treatment (0, 30 or 60 mg/kg). CT density analysis of the lungs was performed on monthly acquired micro-CT images. After 39 weeks, lungs were processed to evaluate the fibrotic phenotype.

Results: Although the CT density increase correlated with the radiation dose, nintedanib did not influence this relationship. Immunohistochemical analysis confirmed the ability of nintedanib to reduce the microscopic fibrotic phenotype, in particular interstitial edema, interstitial and perivascular fibrosis and inflammation, and vasculitis.

Conclusions: Nintedanib reduces radiation-induced lung fibrosis after partial lung irradiation without adverse effects, however, noninvasive CT imaging measuring electron density cannot be applied for monitoring its effects.

Clinically relevant radiation-induced lung damage (RILD) occurs in 5–15% of patients who undergo radiation therapy of the chest to treat lung cancer, but also breast cancer, lymphomas and other cancers. RILD presents as an inflammation of the lungs and depends on the dose of irradiation used and the amount of lung tissue irradiated [1]. RILD is a dose-limiting side effect of irradiation and is a major dose-limiting toxicity [2]. Dose-volume metrics such as the mean lung dose and the percentage of lung volume receiving a dose of 20 Gy or more (*V*20) are associated with pneumonitis, but their predictive value remains low [3]. Computed tomography (CT) imaging of lung characteristics may contribute to the prediction of pneumonitis and fibrosis and the quest for robust genetic predictors continues [4,5].

Nintedanib is an oral small molecule receptor TKI targeting vascular endothelial growth factor receptor (VEGFR) 1–3, fibroblast growth factor receptor (FGFR) 1–3 and platelet-derived growth factor receptor (PDGF) alpha and beta. Nintedanib in combination with docetaxel is approved for the treatment of locally advanced, metastatic, or locally recurrent lung adenocarcinoma after failure of first-line treatment [6]. Nintedanib is also approved for the treatment of patients with idiopathic pulmonary fibrosis (IPF) that is characterized by progressive fibrosis of the lung parenchyma [7]. Nintedanib interferes with central processes in fibrosis such as fibroblast proliferation, migration and differentiation, and the secretion of extracellular matrix proteins [8]. Moreover, nintedanib has shown consistent anti-fibrotic and anti-inflammatory activity in animal models of lung fibrosis [9]. Retrospective studies

☆ This study was presented as an oral presentation at the 16th World Lung Cancer Conference, Denver, CO, USA, September 6–9, 2015 and at the European Cancer Congress (ECCO 18 – ESMO 40), Vienna, Austria, September 25–29, 2015.

* Corresponding author at: MAASTRO, University Maastricht Medical Center, GROW Research Institute, UNS 50/23, 6200 MD Maastricht, The Netherlands.
E-mail address: ludwig.dubois@maastrichtuniversity.nl (L. Dubois).

http://dx.doi.org/10.1016/j.radonc.2017.07.014
0167-8140/

demonstrate that idiopathic pulmonary fibrosis (IPF) is a high risk factor for the development of severe radiation pneumonitis [10].

The aim of the present study was to explore the potential efficacy (quantitative non-invasive CT imaging and semi-quantitative histology as primary and secondary endpoint, respectively) and tolerability of nintedanib in reducing lung fibrosis in a mouse model of RILD.

Materials and methods

Endpoints

The primary endpoint of the study was quantitative non-invasive CT imaging of fibrosis development and the secondary endpoint was semi-quantitative histology for fibrosis 39 weeks post irradiation.

General study design

Adult C57Bl/6 male mice (n = 266) were irradiated with a single fraction radiation dose of 0, 4, 8, 12, 16 or 20 Gy using 5-mm circular parallel-opposed fields (225 kVp, with 0.3 mm added Cu filtration) targeting the upper right lung with a precision image-guided small animal irradiator (XRAD-225Cx, PXI Inc, North Branford, CT, USA) sparing heart and spine based on micro-CT (80 kVp, 2.5 mA, with 2 mm added Al filtration) images from an integrated imaging panel, acquired at a resolution of 100 μm. Irradiation and imaging protocols, dose calculations, deformable registration and image analysis have been previously described in detail [11]. Mice were randomized and one week *after* irradiation, nintedanib was administered once daily (0, 30 or 60 mg/kg) by oral gavage, for a total of 39 weeks (Suppl. Table 1). Micro-CT imaging to assess changes in electron density was repeated on a monthly basis with in total 10 imaging sessions resulting in a cumulative skin dose of approximately 39 cGy. Animals were monitored on a daily basis for signs of compromised health and were weighted before the start of each imaging session. At the end of the experiment, lungs were removed and processed for histological evaluation of the fibrotic phenotype. The general design of the study is outlined in Fig. 1. The study was approved by the Animal Ethical Committee of the University of Maastricht (number 2012-006).

Immunohistochemical staining and analysis

Five-micrometer thick sections were deparaffinized and rehydrated to distilled water. Sections were routinely stained for hematoxylin and eosin (H&E) by consecutive incubation with hematoxylin (10 min, Klinipath), warm tap water (10 min), distilled water wash and eosin solution (3–5 min, VWR). Sections were stained for collagen using a Masson's trichrome stain (Sigma–Aldrich) with Weigert's iron hematoxylin (10 min), warm tap water (10 min), distilled water wash followed by a Biebrich scarlet-acid fuchsin stain (10–15 min), distilled water wash followed by differentiation in phosphomolybdic–phosphotungstic acid solution (10–15 min), aniline blue solution (5–10 min), a rinse in distilled water and 1% acetic acid solution (2–5 min). Consecutive sections were additionally stained for fibrin using an elastic Von Giesson stain (Sigma–Aldrich) with elastic stain solution (10 min), a rinse in deionized water followed by differentiation in ferric chloride solution, a rinse in tap water, 95% alcohol, deionized water followed by van Giesson solution (1–3 min). All sections were dehydrated to xylene through different alcohol incubations and mounted with resinous mounting medium.

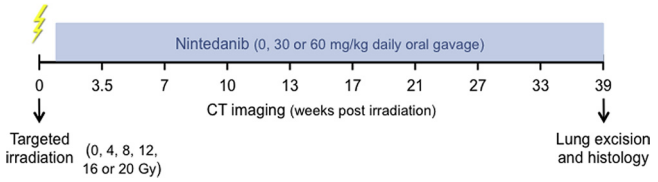

Fig. 1. Study design.

All sections were analyzed in a blinded manner by an experienced lung pathologist (BioGenetics Research Laboratories, Inc., P.S., WA, USA) and scored for (1) alveolar wall thickness, (2) interstitial edema, (3) interstitial fibrosis and inflammation, (4) peribronchial fibrosis and inflammation, (5) perivascular fibrosis and inflammation, (6) increased alveolar macrophages, (7) increased interstitial macrophages, (8) atelectasis (multifocal), (9) alveolar proteinaceous debris (resolved edema), (10) vasculitis (lymphohistiocytic), (11) lymphoid nodules (peribronchiolar), (12) foreign body, pneumonia, (13) bronchioloalveolar adenoma, (14) lymphoreticular infiltration (perivascular), (15) artery tunica media degeneration and (15) bronchioloalveolar carcinoma. The severity of microscopic lesions in each tissue section was graded subjectively from 0 to 4. Grade 0 was indicative for no lesion or normal tissue morphology. Grade 1 indicated minimal histological changes and used for processes where <10% of the tissue was involved. Grade 2 was used for mild histological changes, noticeable but not prominently present in 11–20% of the involved tissue. Grade 3 indicated moderate histological changes and used for the processes in which 21–40% of the tissue was involved. Grade 4 was used for marked, overwhelming histological changes for processes where between 41% and 100% of the tissue was involved [12–14].

Results

Irradiation could be adequately targeted to the right upper lung with sparing of the rest of the chest organs. Dose calculations in the 80% to max irradiated lung region performed with the in house developed validated small animal treatment planning system SmART-Plan [15] for the different irradiation dose groups resulted in similar doses (Suppl. Table 2) between the nintedanib treatment arms and will be referred at as 4, 8, 12, 16 and 20 Gy. The prescribed dose was reached in 9 ± 2% of the total lung volume. Both the irradiation alone and the combination of irradiation with nintedanib treatment were well tolerated. No weight loss was observed and in most cohorts weight increased with age (Fig. 2 and Suppl. Fig. 1). Mortality was observed in 9.9% of the animals, but was completely attributed to application issues during oral gavage, mainly in the first month after the start of compound administration.

CT analysis indicated a dose- and time dependent increase of the lung density in the irradiated area of the right lung, in agreement with the observed pathological characteristics [16]. However, this dose- and time dependent increase of the lung density could not be delayed neither reduced by nintedanib (Fig. 3A and B). A significant ($p < 0.001$) increase in difference between the irradiated and the non-irradiation area of the right lung (delta CT) was observed when comparing 20 Gy with sham-irradiated animals. No significant differences were observed in CT density between the different nintedanib treatment groups with the same radiation dose.

Histological examination of lungs treated with the highest irradiation dose of 20 Gy showed as most obvious findings elevated diffuse alveolar damage, an increase of the alveolar wall thickness, increased alveolar and interstitial macrophages and multifocal atelectasis (Table 1). Additionally, mild interstitial edema, interstitial and perivascular fibrosis and inflammation, alveolar proteinaceous debris, lymphohistiocytic vasculitis, perivascular lymphoreticular infiltration and perivascular artery tunica media

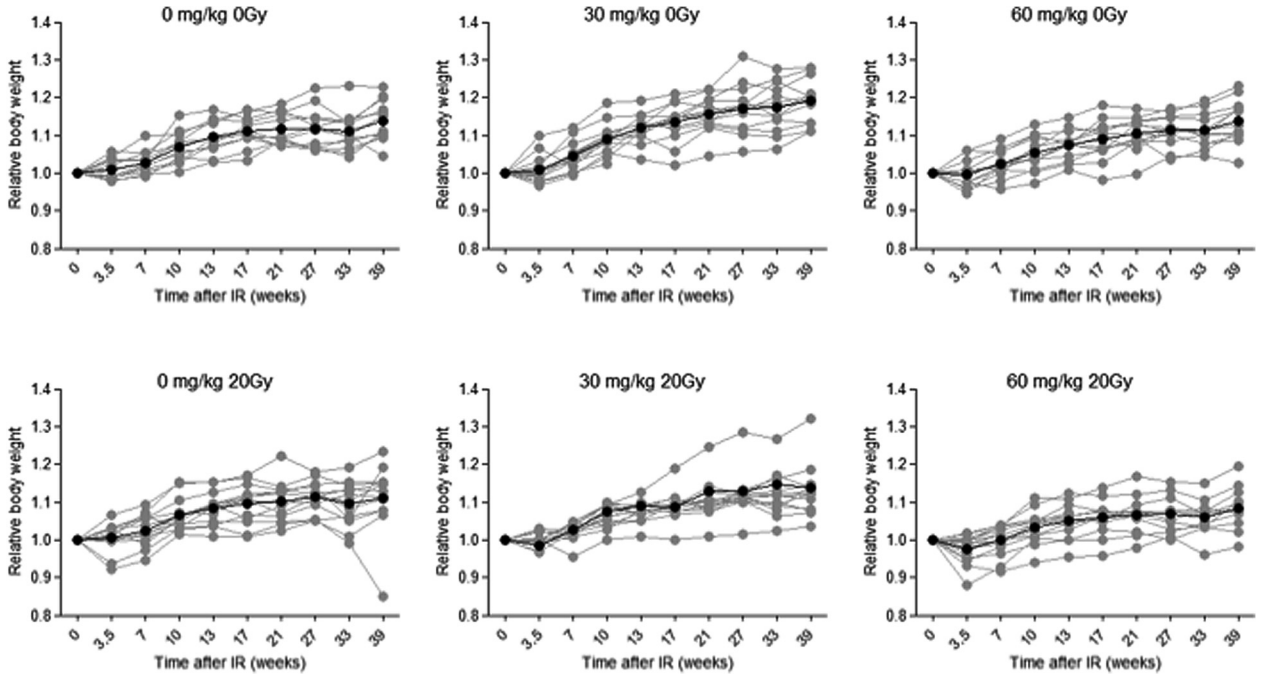

Fig. 2. Changes in relative body weight during the course of the experiment for the indicated experiments. Data (black dots) represent the average of at least 12 individual (Grey) animals.

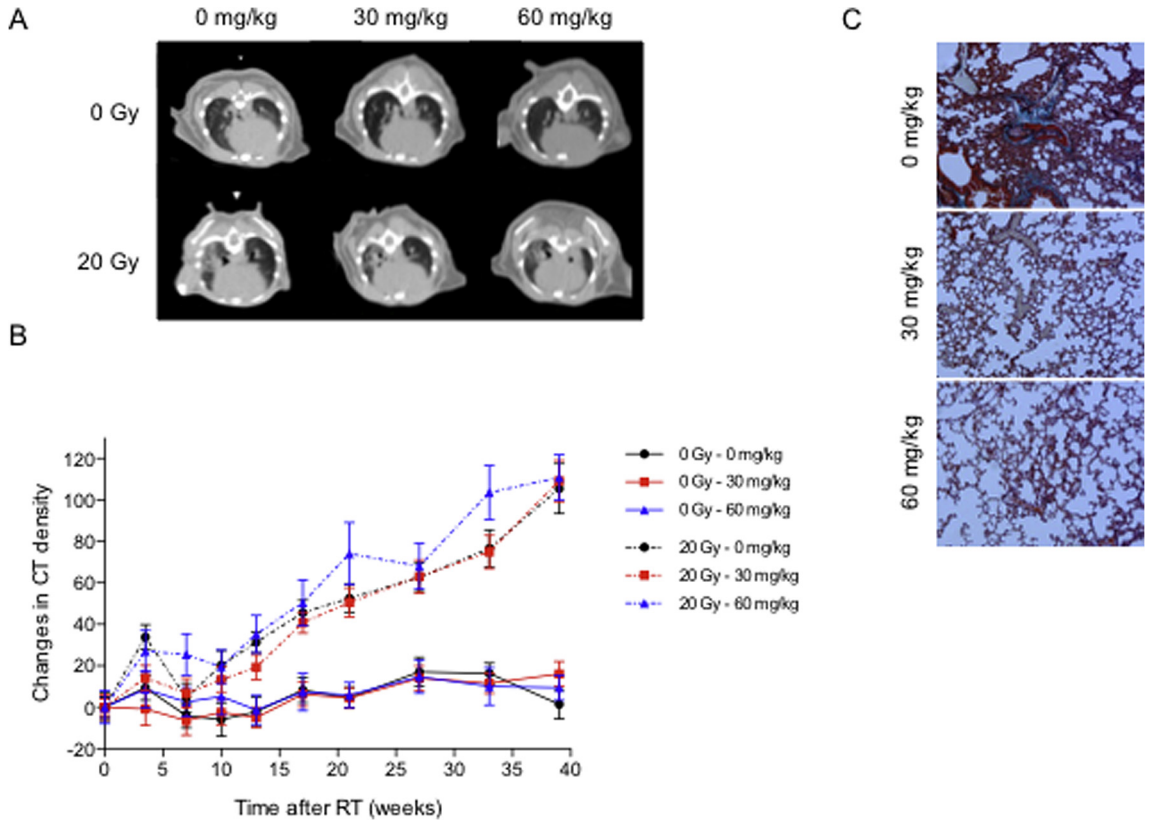

Fig. 3. (A) Representative micro-CT thorax images and (B) effect of nintedanib on the CT density over time of un-irradiated (full lines) and irradiated (20 Gy; dashed lines) animals for 0, 30 or 60 mg/kg nintedanib treatment. (C) Representative Masson's trichrome stainings of the affected lung area 39 weeks after irradiation (20 Gy) treated with 0, 30 or 60 mg/kg nintedanib. Collagen is stained in blue, nuclei are purple and cytoplasm is pink. Data represent the mean ± standard deviation of at least 12 individual animals.

Table 1
Average semi-quantitative histological score of the irradiated lung area 39 weeks after irradiation for 14 different pathological characteristics.

Nintedanib (mg/kg)	0						30						60					
Radiation dose (Gy)	0	4	8	12	16	20	0	4	8	12	16	20	0	4	8	12	16	20
Alveolar wall thickness	0.6	0	1.0	1.1	1.1	1.3	0.8	0.7	0.9	1.1	0.9	1.0	0.7	1.0	0.9	1.1	0.9	1.4
Interstitial edema	0	0	0	0	0	0.5	0	0	0	0	0	0	0	0.1	0	0	0	0.3
Interstitial fibrosis and inflammation	0	0	0	0	0.2	0.2	0	0	0	0	0	0	0	0	0	0	0	0
Perivascular fibrosis and inflammation	0	0	0	0	0.2	0.2	0	0	0	0	0	0	0	0	0	0	0	0
Increased alveolar macrophages	0.7	0.3	1.0	1.2	0.9	1.5	0.6	0.7	0.9	1.1	0.9	1.0	1.0	1.0	0.7	1.2	0.9	1.5
Increased interstitial macrophages	1.2	0	1.0	1.0	1.1	1.5	0.8	0.7	0.9	1.1	0.9	1.0	1.0	0.9	0.7	1.2	0.9	1.6
Multifocal, atelectasis	1.2	1.3	1.5	1.1	1.1	1.4	0.8	0.8	0.9	1.1	0.9	1.0	0.9	1.1	0.9	1.4	1.1	1.3
Alveolar proteinaceous debris, resolved edema	0.3	0	0	0.2	0.1	0.5	0	0	0	0	0	0	0	0	0	0.1	0	0.1
Vasculitis, lymphohistiocytic	0	0	0	0.5	0.3	0.9	0	0.3	0.1	0	0	0	0	0	0	0	0	0
Lymphoid nodules, peribronchiolar	0.3	0	0.1	0.2	0	0	0	0.1	0	0	0.1	0.3	0.2	0.4	0.1	0.5	0.1	0.6
Foreign body inhalation, pneumonia	0	0	0	0	0	0	0	0	0	0	0.1	0	0.3	0	0	0	0	0.3
Bronchioloalveolar adenoma	0	0	0	0	0	0	0	0.1	0.1	0	0	0	0	0	0	0	0	0
Lymphoreticular infiltration, perivascular	0	0	0.7	0.3	0.2	0.3	0.7	0	0.3	0.7	0.4	0.2	0.4	0.8	0.6	0.9	0.4	1.0
Artery tunica media degeneration	0	0	0	0	0	0.3	0	0	0	0	0	0	0	0	0	0	0	0

degeneration was detected. Nintedanib was able to reduce interstitial fibrosis and inflammation, perivascular fibrosis and inflammation, alveolar proteinaceous debris, resolved edema, vasculitis and lymphohistiocytic infiltrations. This effect was observed at 30 mg/kg and at 60 mg/kg doses, without striking differences between the two dosages (Fig. 3C and Table 1). As expected from its working mechanism, nintedanib did not affect alveolar wall thickness and macrophage involvement. At the higher dose of 60 mg/kg, nintedanib seems to augment peribronchiolar lymphoid nodules and lymphoreticular infiltration (Table 2).

Discussion

Radiation-induced lung damage (RILD) is a dose-limiting toxicity for high-dose radiotherapy of lung cancer [1–3]. It is a multifactorial process that involves a cascade of cytokines and growth factors, including repair and migration of many cells in the lungs and its vasculature [1]. Recently, it has also become established that the heart and the lungs are integral functional organs that should be considered together to understand RILD in more detail [17,18]. Genetic factors as well as life-style such as smoking and the characteristics of the lungs all have a role in the susceptibility and the severity of RILD [1–3].

At present, no specific preventive medication or treatment for RILD is available. Amifostine was shown to prevent RILD in preclinical experiments as well as in human studies, but due to concerns of tumor protection and side effects, this medication has not been approved for this indication [19]. Rodent studies and retrospective series in patients suggest that captopril, an angiotensin-converting enzyme (ACE) inhibitor attenuating cardio-pulmonary radiation damage [17,18], may mitigate RILD through its effects on the heart, the blood vessels and repair mechanisms [18,20]. Unfortunately, a prospective trial in non-small cell cancer (NSCLC) patients investigating captopril has been closed early due to lack of accrual [21]. Imatinib, a small molecule receptor tyrosine kinase inhibitor (TKI), targeting the platelet-derived growth factor receptors (PDGFR) alpha and beta and the stem cell factor receptor c-Kit, reduced radiation-induced lung fibrosis in mice with only limited effects against acute inflammation [22]. Strategies that mitigate RILD in experimental models include stem cell therapy, cyclooxygenase (COX)-2 inhibitors, imatinib and captopril, but none of them have been introduced in standard practice [18,21–23]. A drug that could both have a beneficial effect on NSCLC and prevent RILD would be of obvious value.

In the present study, we have shown that nintedanib, a receptor TKI approved for the treatment of metastatic NSCLC and IPF, reduced radiation-induced fibrosis, interstitial edema and vasculitis in a preclinical model of RILD, independent of the tested dosage. As nintedanib interferes with central processes in fibrosis such as fibroblast proliferation, migration and differentiation, and the secretion of extracellular matrix proteins, the findings of our preclinical study are consistent with the mode of action of nintedanib [8]. Also consistent with its mode of action, nintedanib did not affect alveolar wall thickness and macrophage involvement. As

Table 2
Differences in histological score of Table 1 of the affected lung area 39 weeks after treatment between the control group and the treatment groups with nintedanib at 30 mg/kg and 60 mg/kg.

Nintedanib	Δ30						Δ60					
Radiation dose (Gy)	0	4	8	12	16	20	0	4	8	12	16	20
Alveolar wall thickness	0.2	0.7	−0.1	0.0	−0.2	−0.3	0.1	1,0	−0.1	0.0	−0.2	0.1
Interstitial edema	0.0	0.0	0.0	0.0	0.0	−0.5	0.0	0.1	0.0	0.0	0.0	−0.2
Interstitial fibrosis and inflammation	0.0	0.0	0.0	0.0	−0.2	−0.2	0.0	0.0	0.0	0.0	−0.2	−0.2
Perivascular fibrosis and inflammation	0.0	0.0	0.0	0.0	−0.2	−0.2	0.0	0.0	0.0	0.0	−0.2	−0.2
Increased alveolar macrophages	−0.1	0.4	−0.1	−0.1	0.0	−0.5	0.3	0.7	−0.3	0.0	0.0	0.0
Increased interstitial macrophages	−0.4	0.7	−0.1	0.1	−0.2	−0.5	−0.2	0.9	−0.3	0.2	−0.2	0.1
Multifocal, atelectasis	−0.4	−0.5	−0.6	0.0	−0.2	−0.4	−0.3	−0.2	−0.6	0.3	0.0	−0.1
Alveolar proteinaceous debris, resolved edema	−0.3	0.0	0.0	−0.2	−0.1	−0.5	−0.3	0.0	0.0	−0.1	−0.1	−0.4
Vasculitis, lymphohistiocytic	0.0	0.3	0.1	−0.5	−0.3	−0.9	0.0	0.0	0.0	−0.5	−0.3	−0.9
Lymphoid nodules, peribronchiolar	−0.3	0.1	−0.1	−0.2	0.1	0.3	−0.1	0.4	0.0	0.3	0.1	0.6
Foreign body inhalation, pneumonia	0.0	0.0	0.0	0.0	0.1	0.0	0.3	0.0	0.0	0.0	0.0	0.3
Bronchioloalveolar adenoma	0.0	0.1	0.1	0.0	0.0	0.0	0.0	0.0	0.0	0.0	0.0	0.0
Lymphoreticular infiltration, perivascular	0.7	0.0	−0.4	0.4	0.2	−0.1	0.4	0.8	−0.1	0.6	0.2	0.7
Artery tunica media degeneration	0.0	0.0	0.0	0.0	0.0	−0.3	0.0	0.0	0.0	0.0	0.0	−0.3

A reduction in the pathologic score is depicted as negative value and an aggravation as positive value.

expected with the used doses, the drug, which was given once daily for 9 months, was very well tolerated. This may be related to the delivery of a highly localized radiation dose with a high-precision, X-ray guided small animal irradiation device. The radiation dose distribution therefore is a better approximation to that in patients and could spare the vast majority of the lung and the heart. This contrasts to most preclinical studies for RILD, in which the whole chest or the hemi-thorax was irradiated. As RILD is clearly affected by the volume of the irradiated lung and the heart, we believe that our experimental set-up may be more reliable as a step towards testing an intervention in humans [24].

Lung irradiation studies in mice indicate that pneumonitis and fibrosis can be dissociated from each other and that radiation-induced fibrosis can and does occur without a preceding inflammatory event [25]. Therefore, the selection of the mouse strain in pre-clinical RILD research is important since striking strain-related differences are found in radiation sensitivity of the mouse lung [26]. For example, C57BL/6 mice, which are prone to radiation-induced fibrosis, develop less inflammation than C3H mice, which are susceptible to radiation-induced pneumonitis. Conversely, the inflammation-susceptible mice develop less fibrosis than the fibrosis-prone mice [25,26]. It has been demonstrated that for example glucocorticoids can reduce inflammation but not subsequent fibrosis in the lungs of irradiated animals [26]. In addition, although pneumonitis mostly occurs within the irradiated areas of the lung, it may spread to non-irradiated areas, indicating the involvement of cytokines [1]. It has been hypothesized that radiation depletes critical target cells in the lung, which initiates pneumonitis and/or fibrosis. A major effort has been mounted to identify these targets with the intention of protecting them from radiation damage and thereby preventing or at least minimizing the severity of radiation-induced pneumonitis and fibrosis without compromising tumor cell kill and tumor control. The two most likely candidate target cells are thought to be the type II cells (release of surfactant into alveolus) and the vascular endothelial cells (release of surfactant in blood serum) in a network with fibroblasts, macrophages and lymphocytes. Radiation prompts the release of soluble mediators, such as cytokines (e.g. TGFβ, TNFα, TNFβ, IL-1, IL-2) and growth factors (e.g. PDGF, FGF), which deliver the message between the different cells eventually resulting in the pathology of radiation pneumonitis and fibrosis [1]. Pro-fibrotic macrophages producing TGF-β and IL-13 have been shown to be predominant in lungs of IPF patients [27]. Immune dysregulation has been considered, at least, as a collateral mechanism in the pathogenesis of IPF [28], in line with the immunosuppressive effects of radiation through regulation of TGF-β producing pro-fibrotic macrophages [29]. Nintedanib affects various molecular signaling pathways implicated in the pathogenesis and progression of fibrosis [8]. Animal models of lung fibrosis have been used to demonstrate that nintedanib has a preventive and therapeutic anti-fibrotic effect [9]. In vitro studies suggest that nintedanib exerts its anti-fibrotic activity by inhibiting fibroblast proliferation, migration, transformation and contraction [8,30]. Recently, nintedanib was shown to attenuate pro-fibrotic mediator release from T cells [31] and differentiation of alternatively activated macrophages [32]. These data suggest that the anti-fibrotic effect of nintedanib may be elicited directly by attenuating fibroblast functions or indirectly through the immune system.

Our histological results support the testing of nintedanib in patients irradiated for lung cancer. Two clinical trials testing this hypothesis are currently ongoing (NCT02496585, NCT02452463). However, nintedanib did not affect CT density. This could be explained by the fact that CT density is mostly defined by alveolar wall thickness and macrophage infiltration, characteristics which were not affected by nintedanib. Our data suggest that non-invasive CT imaging to monitor efficacy of anti-fibrotic agents is not recommended. FDG-PET imaging could be an alternative to assess inflammation and fibrosis, since a recent study has shown that FDG lung uptake may be used to assess IPF severity and to predict progression-free survival in these patients [33]. The increased uptake found in IPF patients might be related to a metabolic shift towards increased glycolysis, particularly in fibroblasts [34]. This consistent increase in FDG-PET signal however does not seem to align with the fluctuating macrophage infiltration patterns after irradiation [35], emphasizing the need for better alternatives. Our study nevertheless provides further rationale to investigate nintedanib to reduce radiation-induced fibrosis, not only in the lung, but also in other organs.

Conflicts of interest

Dirk De Ruysscher is in the advisory board of Merck, Pfizer and Bristol-Myers Squibb.

Lutz Wollin is an employee of Boehringer Ingelheim.

Others: No conflicts of interest to report.

Acknowledgements

This work has been funded via an investigator-initiated grant by Boehringer Ingelheim (contract number 43040512). The authors would like to thank Anouk Willemsen, Richard Frijnts, Rik Tinnemans and Inger van Rhijn for their technical assistance during the oral gavages.

Appendix A. Supplementary data

Supplementary data associated with this article can be found, in the online version, at http://dx.doi.org/10.1016/j.radonc.2017.07.014.

References

[1] Cappuccini F, Eldh T, Bruder D, et al. New insights into the molecular pathology of radiation-induced pneumopathy. Radiother Oncol 2011;101:86–92.
[2] Vansteenkiste J, De Ruysscher D, Eberhardt WE, et al. Early and locally advanced non-small-cell lung cancer (NSCLC): ESMO Clinical Practice Guidelines for diagnosis, treatment and follow-up. Ann Oncol 2013;24:vi89–98.
[3] Appelt AL, Vogelius IR, Farr KP, Khalil AA, Bentzen SM. Towards individualized dose constraints: adjusting the QUANTEC radiation pneumonitis model for clinical risk factors. Acta Oncol 2014;53:605–12.
[4] Defraene G, van Elmpt W, Crijns W, Slagmolen P, De Ruysscher D. CT characteristics allow identification of patient-specific susceptibility for radiation-induced lung damage. Radiother Oncol 2015;117:29–35.
[5] Kerns SL, West CM, Andreassen CN, et al. Radiogenomics: the search for genetic predictors of radiotherapy response. Future Oncol 2014;10:2391–406.
[6] Reck M, Kaiser R, Mellemgaard A, et al. Docetaxel plus nintedanib versus docetaxel plus placebo in patients with previously treated non-small-cell lung cancer (LUME-Lung 1): a phase 3, double-blind, randomised controlled trial. Lancet Oncol 2014;15:143–55.
[7] Bonella F, Stowasser S, Wollin L. Idiopathic pulmonary fibrosis: current treatment options and critical appraisal of nintedanib. Drug Des Devel Ther 2015;9:6407–19.
[8] Wollin L, Wex E, Pautsch A, et al. Mode of action of nintedanib in the treatment of idiopathic pulmonary fibrosis. Eur Respir J 2015;45:1434–45.
[9] Wollin L, Maillet I, Quesniaux V, Holweg A, Ryffel B. Antifibrotic and anti-inflammatory activity of the tyrosine kinase inhibitor nintedanib in experimental models of lung fibrosis. J Pharmacol Exp Ther 2014;349:209–20.
[10] Ozawa Y, Abe T, Omae M, et al. Impact of preexisting interstitial lung disease on acute, extensive radiation pneumonitis: retrospective analysis of patients with lung cancer. PLoS One 2015;10:e0140437.
[11] Granton PV, Dubois L, van Elmpt W, et al. A longitudinal evaluation of partial lung irradiation in mice by using a dedicated image-guided small animal irradiator. Int J Radiat Oncol Biol Phys 2014;90:696–704.
[12] Brayton CF, Treuting PM, Ward JM. Pathobiology of aging mice and GEM: background strains and experimental design. Vet Pathol 2012;49:85–105.
[13] Shackelford C, Long G, Wolf J, Okerberg C, Herbert R. Qualitative and quantitative analysis of nonneoplastic lesions in toxicology studies. Toxicol Pathol 2002;30:93–6.

[14] ten Hallers EJ, Jansen JA, Marres HA, Rakhorst G, Verkerke GJ. Histological assessment of titanium and polypropylene fiber mesh implantation with and without fibrin tissue glue. J Biomed Mater Res A 2007;80:372–80.
[15] van Hoof SJ, Granton PV, Verhaegen F. Development and validation of a treatment planning system for small animal radiotherapy: SmART-Plan. Radiother Oncol 2013;109:361–6.
[16] Grosse C, Grosse A. CT findings in diseases associated with pulmonary hypertension: a current review. Radiographics 2010;30:1753–77.
[17] Ghobadi G, van der Veen S, Bartelds B, et al. Physiological interaction of heart and lung in thoracic irradiation. Int J Radiat Oncol Biol Phys 2012;84:e639–46.
[18] van der Veen SJ, Ghobadi G, de Boer RA, et al. ACE inhibition attenuates radiation-induced cardiopulmonary damage. Radiother Oncol 2015;114:96–103.
[19] Devine A, Marignol L. Potential of amifostine for chemoradiotherapy and radiotherapy-associated toxicity reduction in advanced NSCLC: a meta-analysis. Anticancer Res 2016;36:5–12.
[20] Kharofa J, Cohen EP, Tomic R, Xiang Q, Gore E. Decreased risk of radiation pneumonitis with incidental concurrent use of angiotensin-converting enzyme inhibitors and thoracic radiation therapy. Int J Radiat Oncol Biol Phys 2012;84:238–43.
[21] Small Jr W, James JL, Moore TD, et al. Utility of the ACE inhibitor captopril in mitigating radiation-associated pulmonary toxicity in lung cancer: results from NRG oncology RTOG 0123. Am J Clin Oncol 2016.
[22] Li M, Abdollahi A, Grone HJ, Lipson KE, Belka C, Huber PE. Late treatment with imatinib mesylate ameliorates radiation-induced lung fibrosis in a mouse model. Radiat Oncol 2009;4:66.
[23] Milas L, Nishiguchi I, Hunter N, et al. Radiation protection against early and late effects of ionizing irradiation by the prostaglandin inhibitor indomethacin. Adv Space Res 1992;12:265–71.
[24] Yahyanejad S, van Hoof SJ, Theys J, et al. An image guided small animal radiation therapy platform (SmART) to monitor glioblastoma progression and therapy response. Radiother Oncol 2015;116:467–72.
[25] Hallahan DE, Geng L, Shyr Y. Effects of intercellular adhesion molecule 1 (ICAM-1) null mutation on radiation-induced pulmonary fibrosis and respiratory insufficiency in mice. J Natl Cancer Inst 2002;94:733–41.
[26] Jackson IL, Vujaskovic Z, Down JD. A further comparison of pathologies after thoracic irradiation among different mouse strains: finding the best preclinical model for evaluating therapies directed against radiation-induced lung damage. Radiat Res 2011;175:510–8.
[27] Prasse A, Pechkovsky DV, Toews GB, et al. A vicious circle of alveolar macrophages and fibroblasts perpetuates pulmonary fibrosis via CCL18. Am J Respir Crit Care Med 2006;173:781–92.
[28] Magnini D, Montemurro G, Iovene B, et al. Idiopathic pulmonary fibrosis: molecular endotypes of fibrosis stratifying existing and emerging therapies. Respiration 2017;93:379–95.
[29] Formenti SC, Demaria S. Combining radiotherapy and cancer immunotherapy: a paradigm shift. J Natl Cancer Inst 2013;105:256–65.
[30] Wollin L, Schuett J, Ostermann A, Herrmann F. The effect of nintedanib on platelet derived growth factor-stimulated contraction of human primary lung fibroblasts. Am J Respir Crit Care Med 2016;193:A2384.
[31] Wollin L, Ostermann A, Brauchle V, Williams C. Nintedanib inhibits pro-fibrotic mediators with relevance in connective tissue disease-associated interstitial lung diseases. Am J Respir Crit Care Med 2017;195:A2450.
[32] Tandon K, Herrmann F, Ayaub E, et al. Nintedanib attenuates the polarization of profibrotic macrophages through the inhibation of thyrosine phosphorylation on Csf1 receptor. Am J Respir Crit Care Med 2017;195:A2397.
[33] Justet A, Laurent-Bellue A, Thabut G, et al. [18F]FDG PET/CT predicts progression-free survival in patients with idiopathic pulmonary fibrosis. Respir Res 2017;18:74.
[34] Maher TM. Aerobic glycolysis and the Warburg effect. An unexplored realm in the search for fibrosis therapies? Am J Respir Crit Care Med 2015;192:1407–9.
[35] Groves AM, Win T, Screaton NJ, et al. Idiopathic pulmonary fibrosis and diffuse parenchymal lung disease: implications from initial experience with 18F-FDG PET/CT. J Nucl Med 2009;50:538–45.